Supporting Information

Cation ordering within the perovskite block of a six-layer Ruddlesden-Popper oxide from layer-by-layer growth – artificial interfaces in complex unit cells

L.Yan[(a)], H. J. Niu[(a)], Giap. V. Duong[(a)], M.R. Suchomel[(a)], J. Bacsa[(a)], P.R. Chalker[(b)], J. Hadermann[(c)], G. van Tendeloo[(c)], M.J. Rosseinsky[(a)*]

(a) Department of Chemistry, University of Liverpool, Liverpool, L69 7ZD, UK
(b) Department of Engineering University of Liverpool Liverpool L69 3GH, UK
(c) Electron Microscopy for Materials Science, University of Antwerp Groenenborgerlaan 171, 2020 Antwerp, Belgium

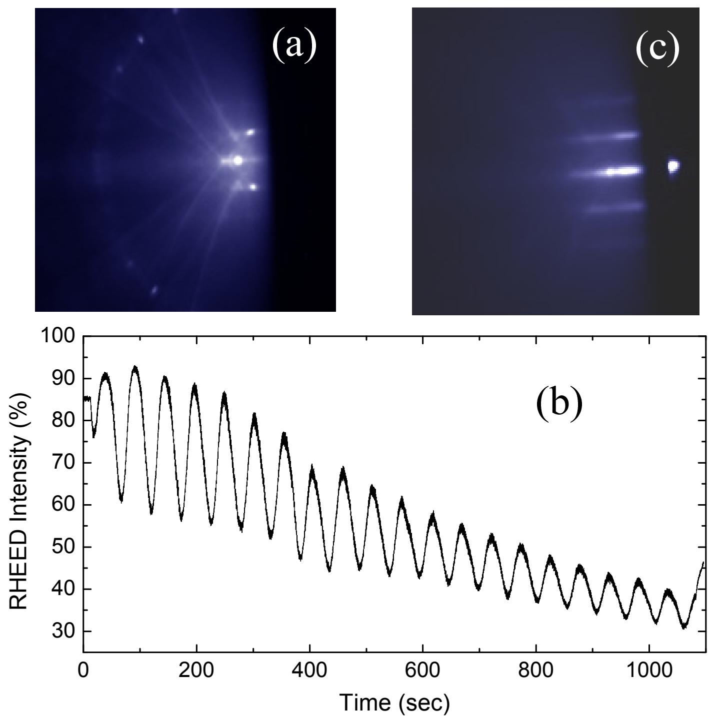

Figure S1. (a) Typical RHEED pattern of (001) STO substrate at room temperature in vacuum ambient. The substrate had been etched with HF-NH_4F (HF 2 wt %) for 30 sec and annealed at 950 ˚C for 3 hours in an air atmosphere.[1] (b) RHEED oscillations of homo-epitaxially grown STO film on a (001) STO substrate at 800 ˚C with oxygen pressure of 2.2×10^{-4} Torr. (c) RHEED pattern of the STO surface after the deposition of the STO layer in (b).

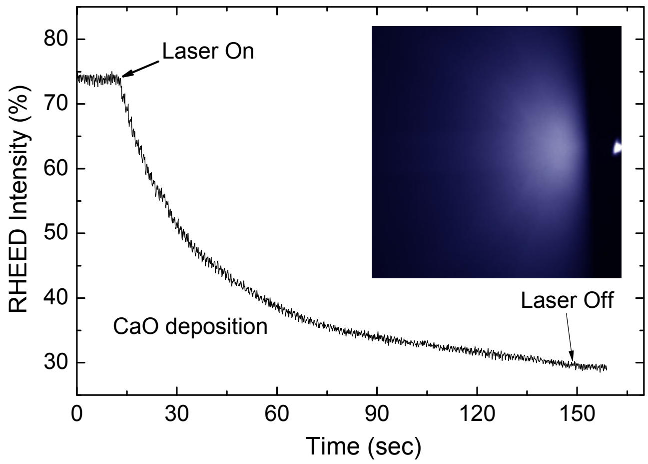

Figure S2. RHEED intensity of a CaO layer deposited directly onto the (001) STO substrate: the inset shows the RHEED pattern after the CaO layer deposition.

Figure S2 shows that the RHEED intensity for a CaO layer deposited directly on a (001) $SrTiO_3$ (STO) substrate (the substrate temperature, oxygen pressure and laser energy and repetition were 700 ˚C, 2.2×10^{-4} Torr, 200 mJ/pulse and 2 Hz, respectively) decreases monotonically. The streaks in the RHEED pattern become gradually indistinct and finally totally disappear as shown in the inset in Figure S2. Crystalline CaO cannot thus be grown epitaxially on STO (001).

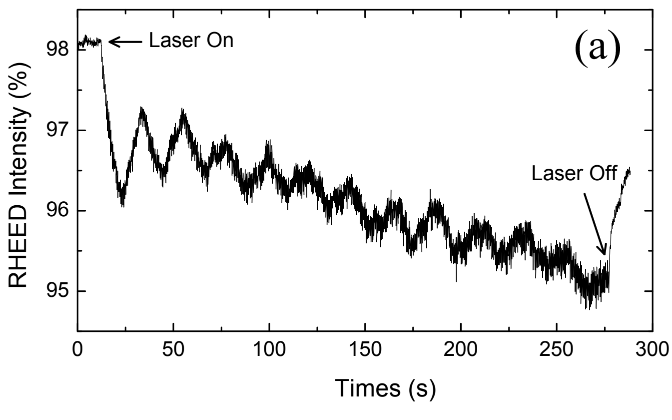

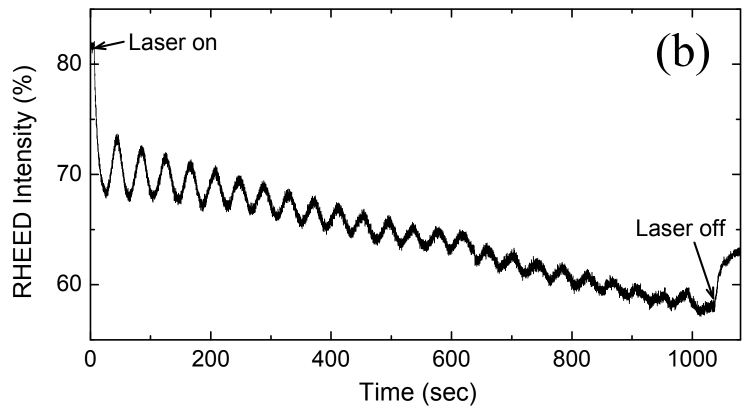

Figure S3 RHEED oscillations of LCMO (a) and CSMO (b) films deposited on (001) STO substrates: the substrate temperature of 700 °C at an oxygen pressure of 4.9×10-4 Torr and the laser energy and repetitions of 200 mJ/pulse and 2 Hz for LCMO and 1 Hz for CSMO, respectively

Introduction of CSMO layer was first investigated through deposition of a $[(CSMO)_2(LCMO)_2(CSMO)_2]$ sequence on a (001) STO substrate as an alternative buffer layer to the six CSMO units discussed in the main text. Figure S4 shows the RHEED oscillations of the final 2 unit cells of the homoepitaxial STO layer and the first set of $[(CSMO)_2(LCMO)_2(CSMO)_2]$ layers deposited on (001) STO at 800 °C with an oxygen pressure of 4.9×10^{-4} Torr. The resulting RHEED pattern indicates that the surface structure of the $[(CSMO)_2(LCMO)_2(CSMO)_2]$ buffer layer is similar to that of the six unit cell CSMO buffer layer. In the following experiments, six unit cells of CSMO were used as the buffer layer for the first CaO layer deposition, because the deposition processing is simple and more easily controlled than for the two-component perovskite buffer layer - this initial layer plays a key role in controlling the subsequent growth process .

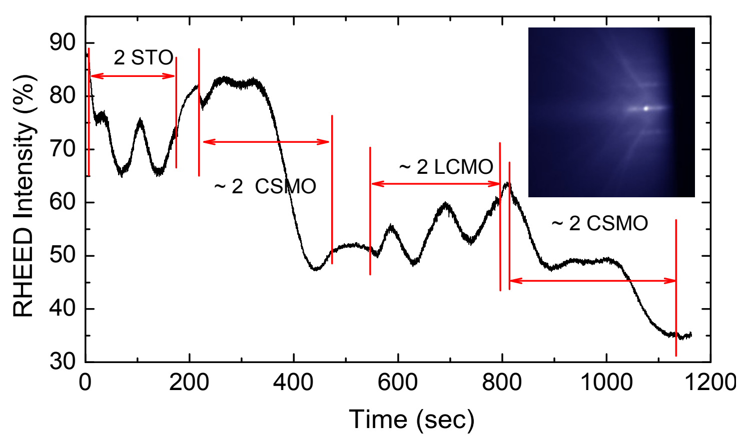

Figure S4. RHEED oscillations of the final STO pre-growth layers and the first $[(CSMO)_2(LCMO)_2(CSMO)_2]$ layers deposited on (001) STO. The inset shows the RHEED pattern after the deposition of the $(CSMO)_2/(LCMO)_2/(CSMO)_2$ layers shown in the RHEED oscillations.

The deposition parameters, such as substrate temperature and oxygen pressure, also affect the film quality. When the n = 6 RP film deposition temperature is below 650 °C, the RHEED oscillations are noisier (Figure S5 vs. Figure 5a), and in particular, the oscillations for the second two CSMO units are not as easily distinguished.

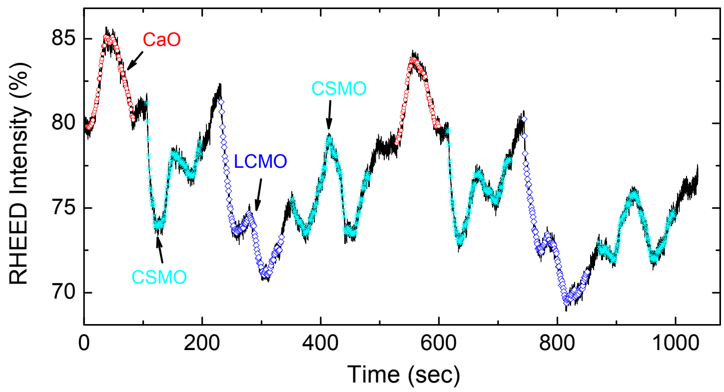

Figure S5. RHEED oscillations of a $CaO/CSMO_2/LCMO_2/CSMO_2$ n = 6 RP deposition at the substrate temperature of 650 °C

As the deposition temperature is lower than 650 °C, the deposited layer cannot be well reconstructed without sufficient thermal energy to drive the required growth processes. When the deposition temperature is above 700 °C, the RHEED oscillations for the CaO layer are not clear enough to determine the number of laser pulses required for the deposition of one monolayer. Figure S6 shows the XRD patterns of the n = 6 RP films deposited at 650, 675 and 700 °C with an oxygen pressure of 4.9×10^{-4} Torr, respectively. The low angle peaks (004) to (008) could not be detected by XRD for the sample deposited at 650 ˚C. The intensity of the (002) peak increases with the deposition temperature.

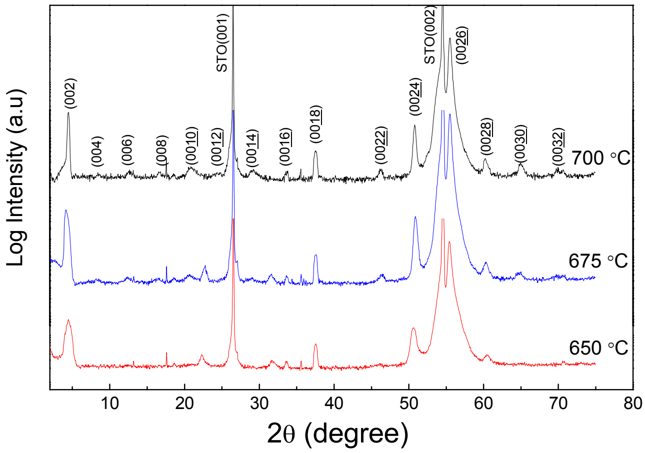

Figure S6. XRD patterns of n = 6 RP films deposited at a substrate temperature of 650, 675 and 700 °C, respectively.

Figure S7 shows the XRD patterns of the *n* = 6 RP films deposited at 700 °C with oxygen pressure from 8×10^{-5}, 2.6×10^{-4} and 4.9×10^{-4} Torr, respectively. There are no low angle (004) to (008) reflections in the XRD pattern in the sample deposited at 8×10^{-5} Torr. The intensity of the (002) peak increases with oxygen pressure. CaO may be more volatile at low pressure than at high oxygen pressure, so that the sample deposited at low pressure is of low quality. However, if the oxygen pressure is high than 4.9×10^{-4} Torr, the plume density focused on the substrate is not uniform enough over large areas and the deposition rate may be different from centre to the edge of the sample. Even though the growth mode can be kept 2-dimensional at high oxygen pressure over a small area, the uneven growth rate produces a sample with low uniformity.

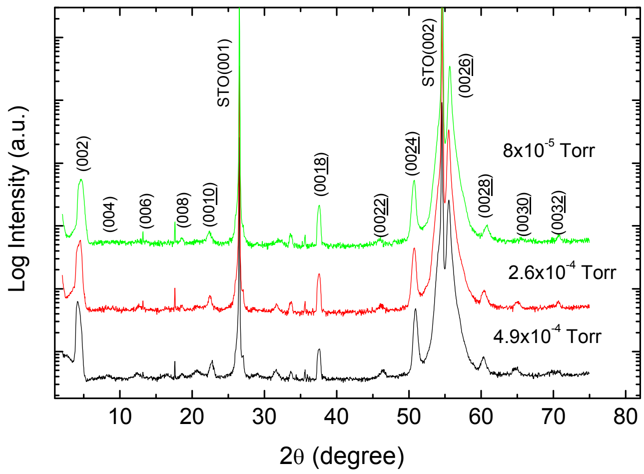

Figure S7. XRD patterns of *n* = 6 RP films deposited at 700 °C with oxygen pressure of 8×10^{-5}, 2.6×10^{-4} and 4.9×10^{-4} torr, respectively.

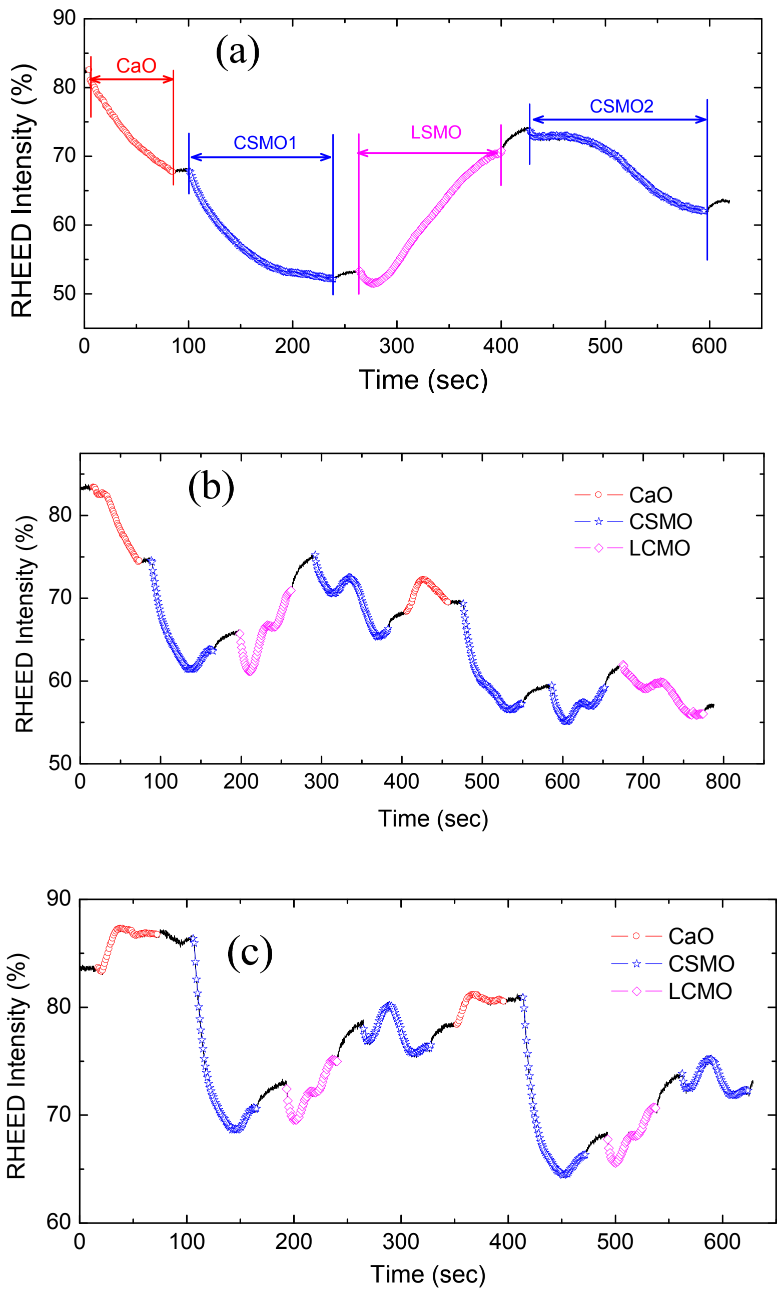

Figure S8. RHEED oscillations of (a) 1st, (b) 2nd to 3rd and (c) 4th to 5th period of $[CaO/(CSMO)_2(/LCMO)_2/(CSMO)_2]_{31}$ during the deposition process of sample **B**.

The deposition process for the targeted $CaO/(CSMO)_2/(LCMO)_2/(CSMO)_2$ n = 6 RP film on the (001) STO substrate can be briefly summarized as requiring the following steps, 1) Substrate treatments. 2) Homo-epitaxial deposition of STO buffer layer. 3) six unit cells CSMO buffer layer deposition. 4) First period of $CaO/(CSMO)_2/(LCMO)_2/(CSMO)_2$ deposition. 5) Repetition of the deposition processing of $CaO/(CSMO)_2/(LCMO)_2/(CSMO)_2$

n times, where $n \approx 30$ here. The route map of the deposition process is graphically represented in Figure S9.

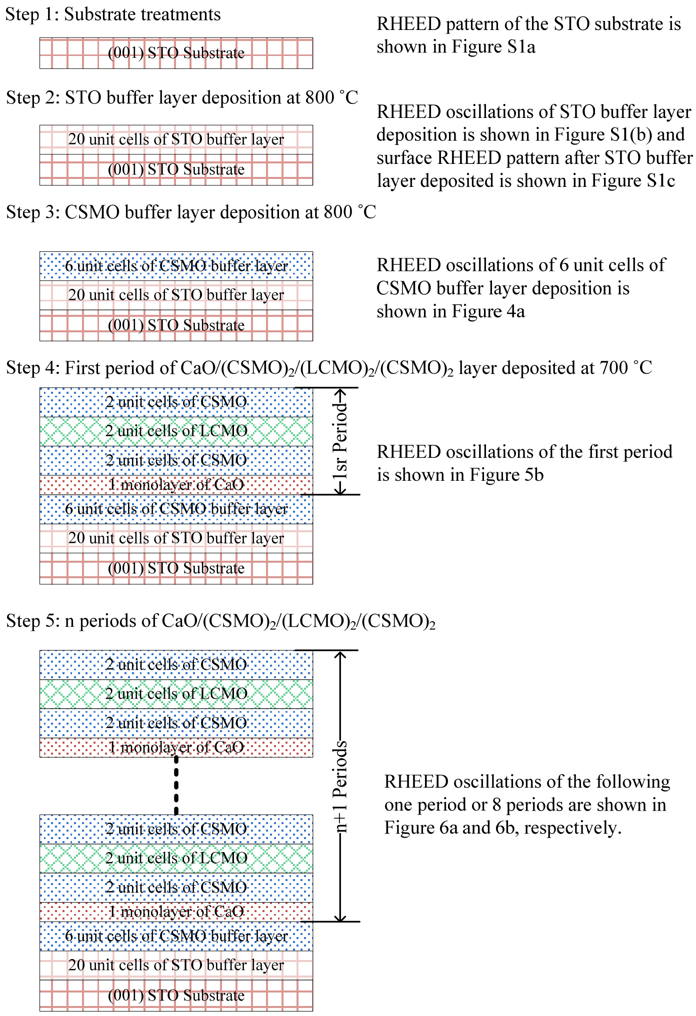

Figure S9. Deposition process of the $CaO[(CSMO)_2/(LCMO)_2/(CSMO)_2]$ n = 6 RP film

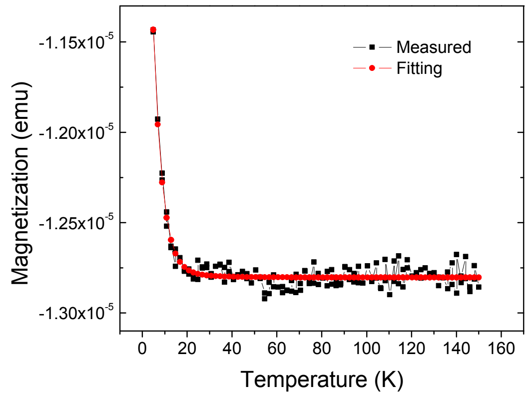

Figure S10. Temperature dependence of magnetization of the STO substrate at a measuring field of 500 Oe. The red line was fitted from the original magnetization data and it was used as the background signal for the n = 6 RP, CSMO and LCMO films.

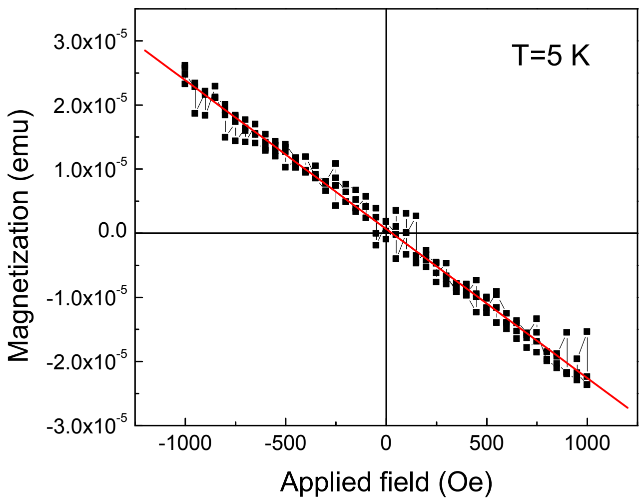

Figure S11. Hysteresis loop of the STO substrate at 5 K.

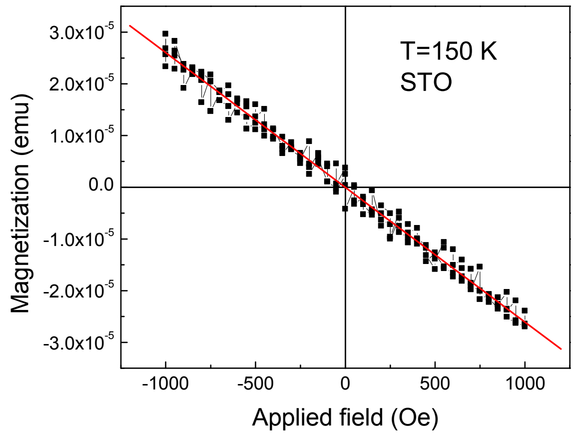

Figure S12. Hysteresis loop of the STO substrate at 150 K, used as the background signal.

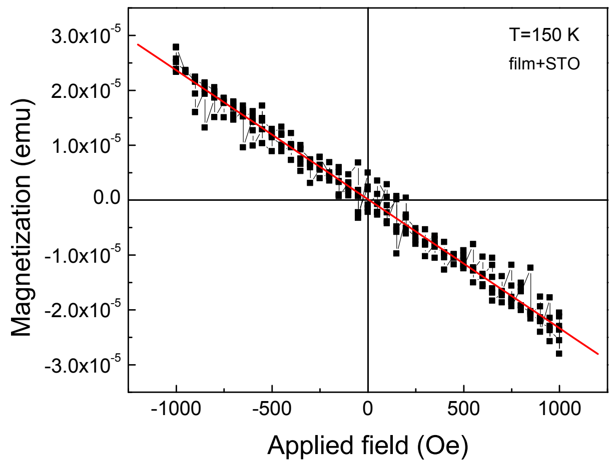

Figure S13 Hysteresis loop of the CSMO-LCMO n = 6 RP film with a thickness of 83 nm at 150 K.

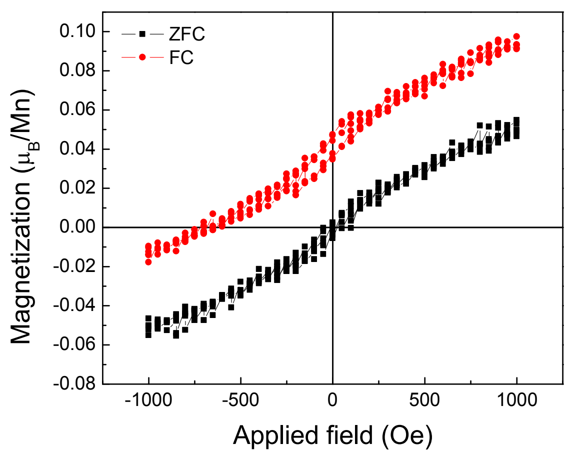

Figure S14. Hysteresis loops of the 86 nm thickness LCMO film deposited on (001) STO under FC and ZFC conditions at 5 K.

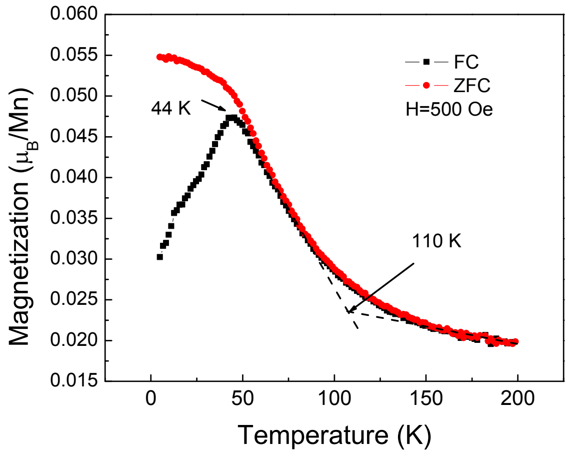

Figure S15. Temperature dependence of the magnetization of 86 nm thickness LCMO film deposited on (001) STO under FC and ZFC conditions.

References

(1) (a) Kawasaki, M.; Takahashi, K.; Maeda, T.; Tsuchiya, R.; Shinohara, M.; Ishiyama, O.; Yonezawa, T.; Yoshimoto, M.; Koinuma, H. *Science* **1994**, *266*, 1540-1542. (b) Rijnders , G. J. H. M.; Koster, G.; Blank, D. H. A.; Rogalla, H. *Materials Science and Engineering B* **1998**, *56*, 223–227. (c) Koster, G.; Kropman, B. L.; Rijnders, G. J. H. M.; Blank, D. H. A.; Rogalla, H. *Appl. Phys. Lett.* **1998**, *73*, 2920-2922.